ARTICLE

Early Stage Solvation of Protonated Methanol by Carbon Dioxide†

Zhi Zhao[a,b‡], Xiang-tao Kong[b‡], Xin Lei[b], Bing-bing Zhang[b,c], Ji-jun Zhao[a], Ling Jiang[b*]

a. Key Laboratory of Materials Modification by Laser, Ion and Electron Beams, Dalian University of Technology, Ministry of Education, Dalian 116024, China
b. State Key Laboratory of Molecular Reaction Dynamics, Collaborative Innovation Center of Chemistry for Energy and Materials, Dalian Institute of Chemical Physics, Chinese Academy of Sciences, Dalian 116023, China
c. State Key Laboratory of Fine Chemicals, Dalian University of Technology, Dalian 116024, China

(Dated: Received on July 10, 2015; Accepted on July 29, 2015)

The solvation of protonated methanol by carbon dioxide has been studied via a cluster model. Quantum chemical calculations of the $H^+(CH_3OH)(CO_2)_n$ (n=1−7) clusters indicate that the first solvation shell of the OH groups is completed at n=3 or 4. Besides hydrogen-bond interaction, the $C_{CO_2}\cdots O_{CO_2}$ intermolecular interaction is also responsible for the stabilization of the larger clusters. The transfer of the proton from methanol onto CO_2 with the formation of the $OCOH^+$ moiety might be unfavorable in the early stage of solvation process. Simulated IR spectra reveal that vibrational frequencies of free O−H stretching, hydrogen-bonded O−H stretching, and O−C−O stretching of CO_2 unit afford the sensitive probe for exploring the solvation of protonated methanol by carbon dioxide. IR spectra for the $H^+(CH_3OH)(CO_2)_n$ (n=1−7) clusters could be readily measured by the infrared photodissociation technique and thus provide useful information for the understanding of solvation processes.

Key words: Methanol, Carbon dioxide, Solvation, Infrared photodissociation spectroscopy, Quantum chemical calculation

I. INTRODUCTION

The study on the hydrogen-bonded (H-bonded) clusters is of fundamental importance in many physical, chemical, atmospheric, and biological sciences in that the nature of these intermolecular interactions and cooperativity effects in larger assemblies govern the aerosol formation and atmospheric nucleation, the hydration of solutes in aqueous solution, and the three-dimensional structures of proteins and nucleic bases [1]. Microhydration studies provide detailed energetic and structural information that is difficult to extract from measurement of bulk solutions. Considerable interest has been focused on water cluster due to the vital role it plays in many biological and physicochemical processes [2]. Since carbon dioxide is one of the major greenhouse gases and plays a significant role in global warming, both theoretical and experimental investigations on CO_2 clusters have received substantial attention during the last two decades [3−8].

Many efforts have been made to address the structure and the energetics of mixed H_2O-CO_2 clusters [3, 4, 7, 9−12]. For instance, infrared photodissociation (IRPD) spectroscopy of the anionic $[(H_2O)_m(CO_2)_n]^-$ (m=1, 2; n=1−4) clusters indicates that the formation of target clusters possibly involves the $(H_2O)_m(CO_2)_n$+e^- collisions followed by electron capture, ion-core formation, solvent migration, and evaporative cooling [10]. For the cationic clusters, time of flight mass spectroscopy of mixed H_2O-CO_2 clusters with single photon ionization at 26.5 eV has demonstrated that the formation of the protonated $H^+(H_2O)_n(CO_2)$ clusters is favored at low CO_2 concentration (*i.e.*, 5% CO_2 partial pressures), whereas the formation of the unprotonated $[(H_2O)_{1,2}(CO_2)_n]^+$ clusters is favored at high CO_2 concentration (*i.e.*, 20% CO_2 partial pressures) [3]. IRPD spectra of the unprotonated $[(H_2O)(CO_2)_n]^+$ clusters show that the first two CO_2 molecules bind to the OH groups of the H_2O^+ ion core and the third and the fourth CO_2 molecules are solvated to the oxygen atom of the H_2O^+ ion core from out of the plane of H_2O^+, completing the first solvation shell at n=4 [12]. Recent high-level quantum chemical calculations of neutral $[(H_2O)_m(CO_2)_n]$ (m=1−3; n=1−12) clusters reveal that seven CO_2 molecules form the first solvent shell of a single H_2O with four CO_2 molecules interacting with the H_2O via Lewis acid-base interactions, two CO_2 interacting with the H_2O by hydrogen bonds, and the seventh CO_2 completing the shell [7].

†Dedicated to Professor Qing-shi Zhu on the occasion of his 70th birthday.
‡These authors contributed equally to this work.
*Author to whom correspondence should be addressed. E-mail: ljiang@dicp.ac.cn

Methanol is the simplest but important one used as clean liquid fuels and ideal solvents in industry, which has received increasing attention because of the presence of both polar and nonpolar moiety. Recently, tunable synchrotron vacuum ultraviolet (VUV) radiation has been used to study small methanol clusters, indicating that the protonated methanol dimer and trimer ($H^+(CH_3OH)_{2,3}$) are the most abundant ion at the different ionization region [13]. It has been inferred that beyond six methanol molecules, the clusters are found to behave similarly to liquid methanol [14, 15]. IRPD spectra of the unprotonated $[(CH_3OH)(CO_2)_n]^+$ (n=1−7) clusters show that the first CO_2 molecule is bonded to the OH group of the CH_3OH^+ ion core and the second and third CO_2 molecules are bonded to the oxygen atom of the CH_3OH^+ ion core [12]. No structural information was reported for the larger $[(CH_3OH)(CO_2)_n]^+$ (n>3) clusters. So far, much less work has been carried out for the interaction of protonated methanol ($H^+(CH_3OH)$) with a number of CO_2. The issue how the excess proton affects solvation motif of $H^+(CH_3OH)$ as compared to CH_3OH^+ remains open.

Herein, we present a study on the solvation of $H^+(CH_3OH)$ by CO_2 via a cluster model. Quantum chemical calculations of the $H^+(CH_3OH)(CO_2)_n$ (n=1−7) clusters indicate that the first solvation shell of the OH groups is completed at n=3 or 4. Simulated IR spectra reveal that vibrational frequencies of free O−H stretching, H-bonded O−H stretching, and O−C−O stretching of CO_2 unit afford the sensitive probe for exploring early stage solvation of protonated methanol by carbon dioxide.

II. THEORETICAL METHODS

Quantum chemical calculations are performed using Gaussian 09 program suite [16]. Initial configurations are built on the basis of the relevant structures reported in the literature. Considering that the interaction of methanol with carbon dioxide could be properly predicted by the M06-2X hybrid functional [1, 8], which is employed for the present calculations. The aug-cc-pVDZ basis set is used for C, H, and O atoms. Tight convergence of the optimization and the self-consistent field procedures is imposed, and an ultrafine grid is used. Relative and dissociation energies include zero-point vibrational energies. Harmonic vibrational frequencies are calculated at the same level. All reported structures are true minima without imaginary vibrational frequencies. Simulated IR spectra are derived from M06-2X/aug-cc-pVDZ harmonic vibrational frequencies and intensities. Harmonic vibrational frequencies are scaled by a factor of 0.948, which is determined by the comparison of simulated vibrational frequencies of O−C−O stretching for CO_2 unit in the $[CH_3OH(CO_2)]^+$ cluster with experimental value [12]. IR stick spectra are convoluted by a Gaussian line shape function with a width of 10 cm^{-1} (FWHM).

III. RESULTS AND DISCUSSION

A. Solvation motifs and IR spectra

Several representative low-lying structures of the $H^+(CH_3OH)(CO_2)_n$ (n=1−7) clusters are presented in Fig.1. The structures are labeled according to the number of CO_2 molecules and relative energies. For each cluster up to n=7, simulated IR spectra of the representative low-lying isomers are shown in Figs.2−8. Harmonic vibrational frequencies and intensities of free O−H stretching, H-bonded O−H stretching, and O−C−O stretching of CO_2 unit for the lowest-lying isomers of $H^+(CH_3OH)(CO_2)_n$ (n=1−7) are listed in Table I.

1. n=1

As illustrated in Fig.1, CO_2 in the lowest energy isomer (labeled 1A) forms one H-bond with one OH group, leaving another OH group free. The optimization of the initial structure with oxygen atom (O_{CO_2}) of CO_2 coordinated to the two hydroxy hydrogen atoms ($H_{hydroxy}$) of methanol converges to isomer 1A. The 1B isomer lies 30.51 kJ/mol higher in energy, in which three H-bonds in-between and three methyl hydrogen atoms (H_{methyl}) of CH_3OH are formed. In the third isomer, 1C, the proton is transferred from methanol onto CO_2, forming the $OCOH^+$ moiety. This isomer lies 127.60 kJ/mol above 1A. Isomer 1C consists of two H-bonds of $O_{CO_2}\cdots H_{hydroxy}$ and oxygen atom ($O_{methanol}$) of methanol with hydrogen atom (H_{OCOH^+}) of the $OCOH^+$ moiety, and one intermolecular interaction between carbon atom (C_{CO_2}) of CO_2 and $O_{methanol}$ atom.

Three main absorption peaks are observed in 1A (Fig.2). The frequency at 3554 cm^{-1} is attributed to the free O−H stretching vibration of methanol (labeled free ν_{OH}) (Table I). The frequencies at 3075 and 3068 cm^{-1} correspond to the H-bonded O−H stretching vibrations (labeled H-bonded ν_{OH}), which converge to one peak in the convoluted spectrum. The peak at 2343 cm^{-1} belongs to the O−C−O stretching vibration for CO_2 unit (labeled ν_{OCO} (CO_2)). Since two OH groups in 1B are free, two peaks at 3570 and 3486 cm^{-1} are observed for free ν_{OH} mode. The ν_{OCO} mode in 1B shows red-shift of 20 cm^{-1} relative to that in 1A. In the proton transferred structure of 1C, three modes of free ν_{OH}, O−C−O stretching for $OCOH^+$ unit (labeled $\nu_{OCO}(OCOH^+)$), and COH bending for $OCOH^+$ unit (labeled δ_{COH}) present around 3574, 3475, 2008, and 1202 cm^{-1}, respectively. The structure 1C lies too high in energy and should not be readily observed in the experiment. Remarkable discrepancy in the simulated IR

DOI:10.1063/1674-0068/28/cjcp1507146

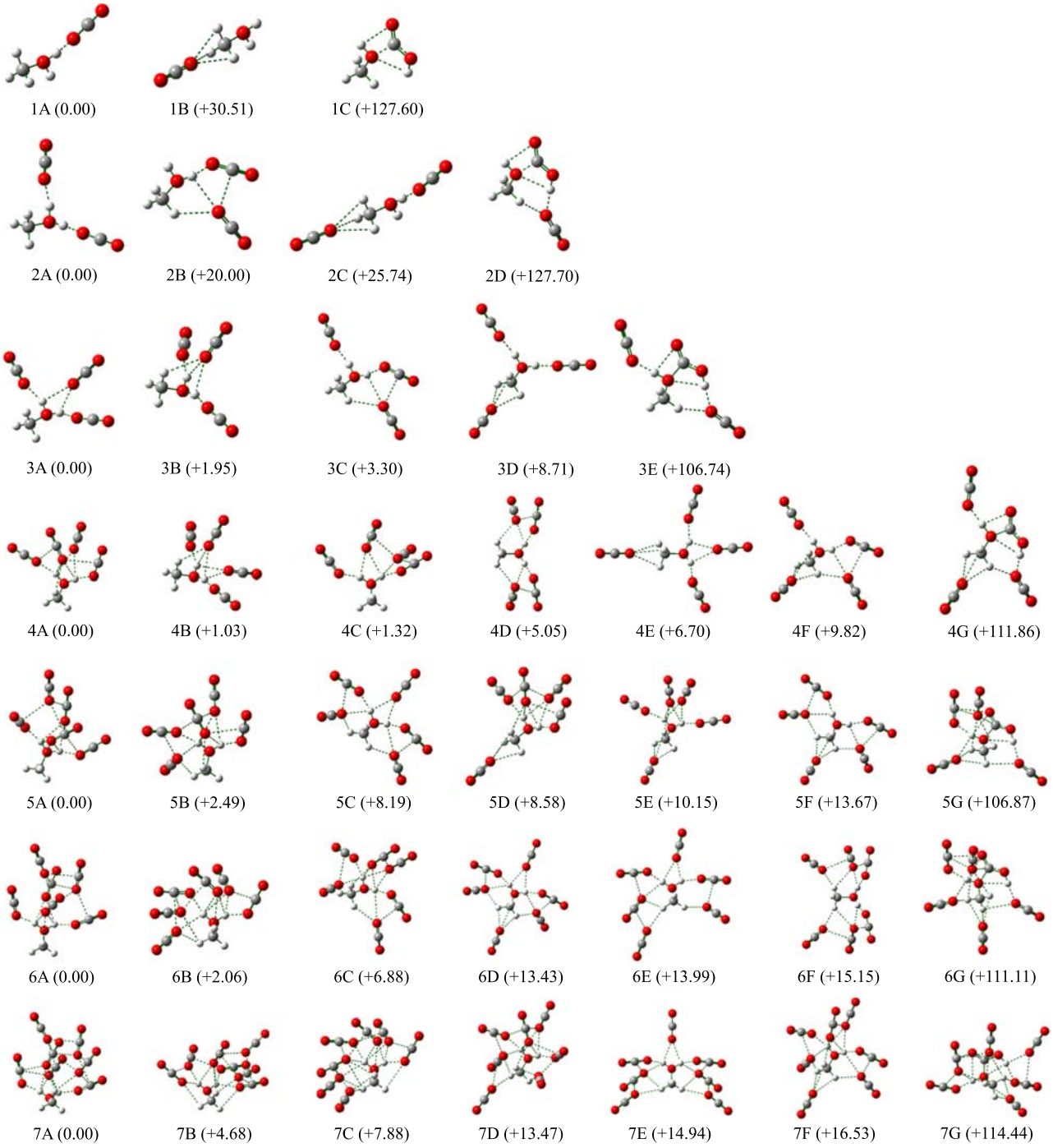

FIG. 1 Optimized structures of the $H^+(CH_3OH)(CO_2)_n$ (n=1−7) clusters. Relative energies are given with unit of kJ/mol in parentheses.

spectra of 1A and 1B suggests that these two isomers could be distinguished in the experiment.

2. n=2

The lowest energy isomer (labeled 2A) is a C_s structure, in which the CO_2 molecules form two H-bonds with the OH groups of the $H^+(CH_3OH)$ cation (Fig.1). In the next energetically low-lying isomer 2B (+20 kJ/mol), the second CO_2 adds to the cluster such that the $O_{CO_2}\cdots H_{hydroxy}$ and $O_{CO_2}\cdots H_{methyl}$ H-bonds and $C_{CO_2}\cdots O_{CO_2}$ intermolecular interaction are formed and one free OH is reserved. The structure of 2C contains the second CO_2 bonded to the H_{methyl} atoms, which lies 25.74 kJ/mol above 2A. In the isomer 2D, the second CO_2 forms two H-bonds

DOI:10.1063/1674-0068/28/cjcp1507146

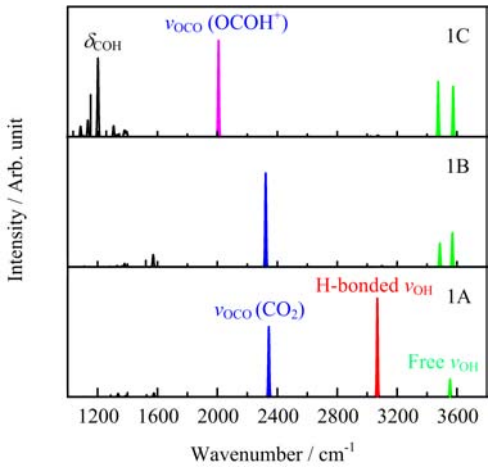

FIG. 2 Simulated IR spectra of the three optimized isomers of $H^+(CH_3OH)(CO_2)$. Assignments of free O−H stretching, H-bonded O−H stretching, O−C−O stretching for CO_2 unit, O−C−O stretching for $OCOH^+$ unit, and COH bending for $OCOH^+$ unit are indicated in green, red, blue, magenta, and dark, respectively.

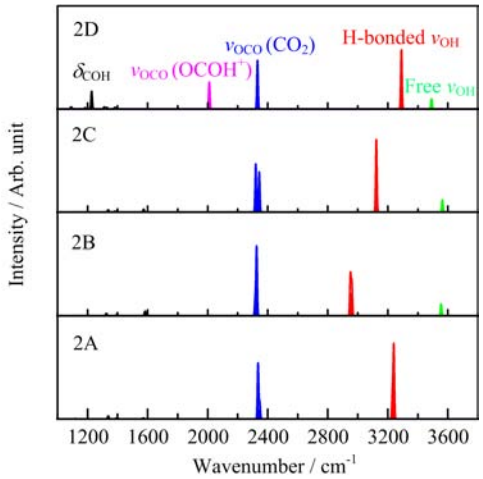

FIG. 3 Simulated IR spectra of the four optimized isomers of $H^+(CH_3OH)(CO_2)_2$. Assignments of free O−H stretching, H-bonded O−H stretching, O−C−O stretching for CO_2 unit, O−C−O stretching for $OCOH^+$ unit, and COH bending for $OCOH^+$ unit are indicated in green, red, blue, magenta, and dark, respectively.

of $O_{CO_2}\cdots H_{OCOH^+}$ and $O_{CO_2}\cdots H_{methyl}$, which lies 127.70 kJ/mol above 2A.

In the simulated IR spectrum of 2A (Fig.3), two sharp peaks centered around 3235 and 2340 cm^{-1} are responsible for H-bonded ν_{OH} and ν_{OCO} (CO_2) modes (Table I), respectively. Both OH groups are solvated by two CO_2, resulting in the absence of free ν_{OH} mode. The structure of 2B releases one OH group free, and then free ν_{OH} mode recovers around 3555 cm^{-1}. The peak of H-bonded ν_{OH} mode in 2B is red-shifted by 280 cm^{-1} with respect to 2A. The ν_{OCO} mode in 2B appears around 2320 cm^{-1}. The isomer 2C gives three

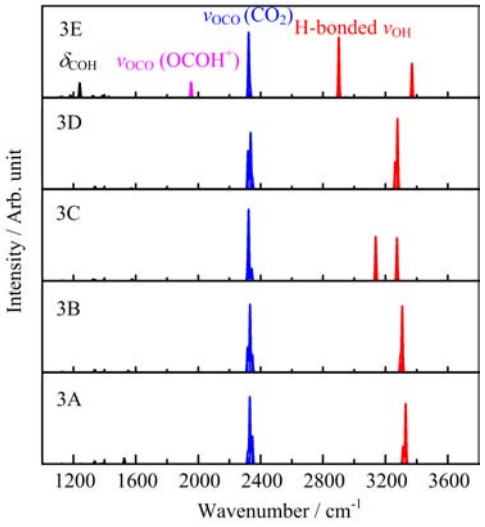

FIG. 4 Simulated IR spectra of the five optimized isomers of $H^+(CH_3OH)(CO_2)_3$. Assignments of free O−H stretching, H-bonded O−H stretching, O−C−O stretching for CO_2 unit, O−C−O stretching for $OCOH^+$ unit, and COH bending for $OCOH^+$ unit are indicated in green, red, blue, magenta, and dark, respectively.

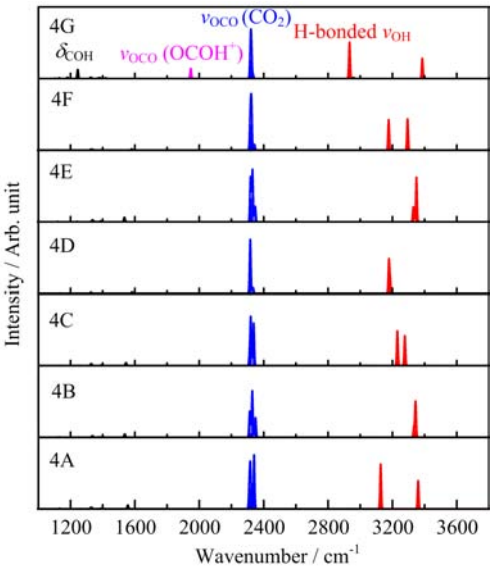

FIG. 5 Simulated IR spectra of the seven optimized isomers of $H^+(CH_3OH)(CO_2)_4$. Assignments of H-bonded O−H stretching, O−C−O stretching for CO_2 unit, O−C−O stretching for $OCOH^+$ unit, and COH bending for $OCOH^+$ unit are indicated in green, red, blue, magenta, and dark, respectively.

main modes analogous to 2B, in which H-bonded ν_{OH} mode in 2C is red-shifted by about 110 cm^{-1} with respect to 2A. Besides these three fundamental modes observed in 2A−2C, the peaks of $\nu_{OCO}(OCOH^+)$ and δ_{COH} modes present in 2D because of the involvement of the $OCOH^+$ moiety.

DOI:10.1063/1674-0068/28/cjcp1507146

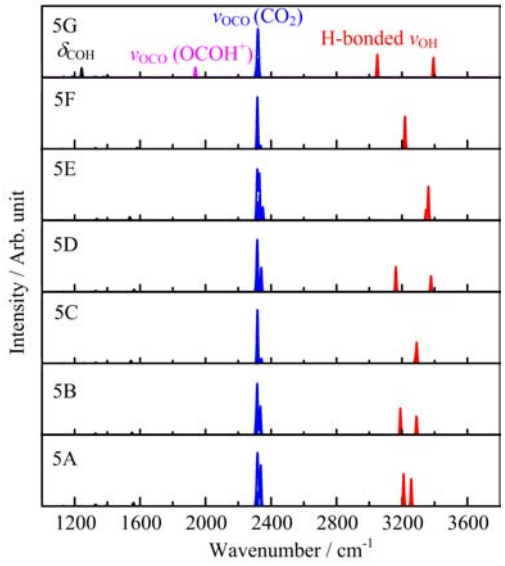

FIG. 6 Simulated IR spectra of the seven optimized isomers of $H^+(CH_3OH)(CO_2)_5$. Assignments of H-bonded O−H stretching, O−C−O stretching for CO_2 unit, O−C−O stretching for $OCOH^+$ unit, and COH bending for $OCOH^+$ unit are indicated in red, blue, magenta, and dark, respectively.

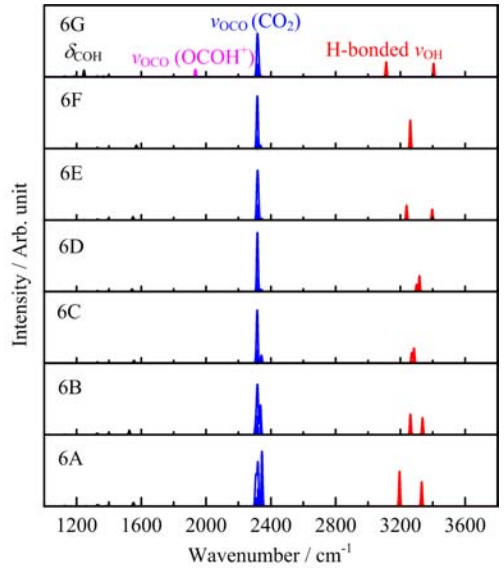

FIG. 7 Simulated IR spectra of the seven optimized isomers of $H^+(CH_3OH)(CO_2)_6$. Assignments of H-bonded O−H stretching, O−C−O stretching for CO_2 unit, O−C−O stretching for $OCOH^+$ unit, and COH bending for $OCOH^+$ unit are indicated in red, blue, magenta, and dark, respectively.

3. n=3

The lowest energy isomer (3A) could be viewed as the derivative of 2A, in which the third CO_2 attaches to two $H_{hydroxy}$ atoms (Fig.1). When the third CO_2 is lifted up to form the $O_{CO_2}\cdots H_{methyl}$ bond, resulting in the structure of 3B, whose energy is elevated by 1.95 kJ/mol. 3C is evolved from 2B, in which the third CO_2 forms one $O_{CO_2}\cdots H_{hydroxy}$ H-bond. The isomer 3D (+8.71 kJ/mol) consists of two $O_{CO_2}\cdots H_{hydroxy}$ H-bonds and three $O_{CO_2}\cdots H_{methyl}$ bonds. As compared to the structure of 2D, the third CO_2 in 3E binds to the OH group and forms one $O_{CO_2}\cdots H_{hydroxy}$ H-bond, which lies 106.74 kJ/mol above 3A.

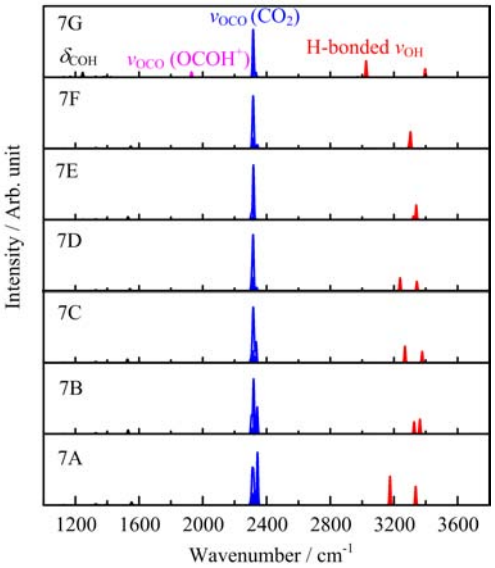

FIG. 8 Simulated IR spectra of the seven optimized isomers of $H^+(CH_3OH)(CO_2)_7$. Assignments of H-bonded O−H stretching, O−C−O stretching for CO_2 unit, O−C−O stretching for $OCOH^+$ unit, and COH bending for $OCOH^+$ unit are indicated in red, blue, magenta, and dark, respectively.

Obvious peaks in the IR spectra of 3A, 3B, and 3D with C_s symmetry are due to H-bonded ν_{OH} and ν_{OCO} (CO_2) modes (Fig.4), in which peak positions are similar to each other except the slight difference in the calculated intensities. Remarkable splitting for the H-bonded ν_{OH} mode in 3C is observed at 3274 and 3138 cm^{-1}, which is due to the broken symmetry. Two additional peaks of $\nu_{OCO}(OCOH^+)$ and δ_{COH} modes also appear in the proton transferred structure of 3E. Free ν_{OH} mode is absent in all the isomers of the n=3 cluster.

4. n=4−7

For the n=4 cluster, the structures of 4A−4C hold the similar feature involved with the CO_2 mainly bonded to the sides of the OH groups (Fig.1), which are almost energetically identical. The CO_2 molecules in the isomers 4D−4F solvate both OH groups and methyl. The highest-lying isomer (4G, +111.86 kJ/mol) contains the $OCOH^+$ moiety, which could be viewed as the derivative of 3E. In the low-energy structures for the n=5−7 clusters, the CO_2 molecules prefer to sol-

DOI:10.1063/1674-0068/28/cjcp1507146

TABLE I Simulated vibrational frequencies (f) and intensities (I) of free O−H stretching, H-bonded O−H stretching, and O−C−O stretching of CO_2 unit for the lowest-lying isomers of $H^+(CH_3OH)(CO_2)_n$ (n=1−7) together with the lowest dissociation energies for the loss of one CO_2 molecule (E_{diss}), CO_2-sovlated O−H bond lengths (R_{O-H}) and Wiberg bond order of the OH moiety (P_{O-H}).

Species	Free ν_{OH}		H-bonded ν_{OH}		ν_{OCO} (CO_2)		E_{diss}/(kJ/mol)	R_{O-H}/Å	P_{O-H}
	f/cm^{-1}	I/(km/mol)	f/cm^{-1}	I/(km/mol)	f/cm^{-1}	I/(km/mol)			
1A	3554	290	3075	155	2343	1151	49.57	0.998	0.56
			3068	1614					
2A			3240	2275	2347	514	42.19	0.989	0.58
			3231	771	2336	1726			
3A			3330	1685	2347	780	23.42	0.989	0.58
			3313	493	2331	1876			
					2318	347			
4A			3360	840	2340	1609	20.70	0.984	0.59
			3127	1331	2318	1092			0.56
					2313	459			
					2310	365			
5A			3257	1020	2337	1537	22.15	0.988	0.58
			3211	1209	2321	992			
					2317	710			
					2313	930			
					2305	70			
6A			3332	868	2345	1954	19.02	0.986	0.58
			3195	1243	2322	446			
					2320	1145			
					2312	549			
					2308	448			
					2305	442			
7A			3337	836	2343	2364	22.37	0.985	0.57
			3176	1300	2319	411			
					2319	899			
					2313	376			
					2310	991			
					2307	247			
					2300	117			

vate the OH groups. The structures with higher symmetry (*i.e.*, 4D, 5C, 6D, and 7F) are predicted to lie about 5−15 kJ/mol above nA. The structures with the $OCOH^+$ moiety (*i.e.*, 5G, 6G, and 7G) still lie too high in energy among each cluster series, implying that the proton transfer might be unfavorable in the early stage of solvation process.

In the simulated IR spectra of 4A−4F (Fig.5), H-bonded ν_{OH} and ν_{OCO} (CO_2) modes are remarkably observed. Additional peaks of $\nu_{OCO}(OCOH^+)$ and δ_{COH} modes present in 4G. Free ν_{OH} mode is absent in all the isomers of n=4. In 4A, the peaks for H-bonded ν_{OH} mode appear at 3360 and 3127 cm^{-1}, which could be resolved in the experiment. The peaks for ν_{OCO} mode in 4A−4G are centered around 2320 cm^{-1}. As depicted in Figs.6−8, simulated IR spectra for n=5−7 exhibit the similar fundamental modes for n=4, indicating the gradually converged solvation of protonated methanol by CO_2 (vide infra).

B. General trend

IR spectra of the lowest-lying isomers for the $H^+(CH_3OH)(CO_2)_n$ (n=1−7) clusters are compared in Fig.9. The lowest dissociation energies for the loss of one CO_2 molecule, CO_2-sovlated O−H bond lengths and Wiberg bond order of the OH moiety are summarized in Table I.

It can be seen from the aforementioned solvation motifs that the CO_2 molecules in the $H^+(CH_3OH)(CO_2)_n$ clusters up to n=7 prefer to bind to the OH groups of methanol rather than methyl side, even though the first solvation shell of the OH groups is completed

DOI:10.1063/1674-0068/28/cjcp1507146

at n=3 or 4. Together with H-bond interaction, the $C_{CO_2}\cdots O_{CO_2}$ intermolecular interaction joins in the stabilization of the larger clusters. The transfer of the proton from methanol onto CO_2 with the formation of the $OCOH^+$ moiety might be unfavorable in the early stage of solvation process. Previous studies on the $[(CH_3OH)(CO_2)_n]^+$ (n=1−3) clusters reveal that the first CO_2 molecule is bonded to the OH group of the unprotonated CH_3OH^+ ion core and the second and third CO_2 molecules are bonded to the oxygen atom of the CH_3OH^+ ion core [12]. Then, solvation pattern of the unprotonated $[(CH_3OH)(CO_2)_n]^+$ (n=1−3) clusters is different from that of the protonated $H^+(CH_3OH)(CO_2)_n$ clusters.

As depicted in Fig.9, the n=1 cluster exhibits three groups of intense absorptions for free ν_{OH}, H-bonded ν_{OH}, and ν_{OCO}, while the n=2−7 clusters feature two modes of H-bonded ν_{OH} and ν_{OCO}. In the n=1−3 clusters, H-bonded ν_{OH} mode appears as a single peak, whose vibrational frequency is blue-shifted from 3070 cm^{-1} to 3320 cm^{-1} with the increase of cluster size, indicating the O−H bond strength of methanol recovers gradually as the number of the CO_2 molecule increases. For n=4−7 clusters, H-bonded ν_{OH} mode presents as doublet peaks with the center around 3200 cm^{-1}. Especially, simulated IR spectra of n=6 and 7 are almost the same. These findings suggest that the solvation of the OH groups of prontonated methanol approaches to be converged around n=3 or 4. The lowest dissociation energy for the loss of one CO_2 molecule for 1A−7A is predicted to be 49.57, 42.19, 23.42, 20.70, 22.15, 19.02, and 22.37 kJ/mol, respectively (Table I), supporting the above-mentioned trend of the solvation. Similar evidence could be obtained from CO_2-sovlated O−H bond lengths and Wiberg bond order (Table I).

IRPD spectroscopy of mass-selected complexes has emerged as a powerful tool for the structural characterization of the gas-phase species [2, 17−22]. Under readily achievable experimental conditions, absorption of single IR photon or multiple IR photons by a cluster can induce a measurable increase in the sequence, resulting in IRPD spectra that closely resemble linear absorption spectra. Compared with the conventional vibrational spectroscopy, IRPD has advantages of high selectivity, high sensitivity and being a background-free consequence technique.

Considering that free O−H stretching, H-bonded O−H stretching, and O−C−O stretching of CO_2 unit have been successfully resolved in the IRPD spectra of a series of mass-selected clusters radiated by optical parametric oscillator/optical parametric amplifier (OPO/OPA) table-top laser system or infrared free electron laser (IR-FEL) source [2, 10, 12, 22−25], the predicted IR spectra for the $H^+(CH_3OH)(CO_2)_n$ (n=1−7) clusters could be readily measured by the IRPD technique and thus afford useful information for the understanding of early stage solvation of protonated methanol by carbon dioxide.

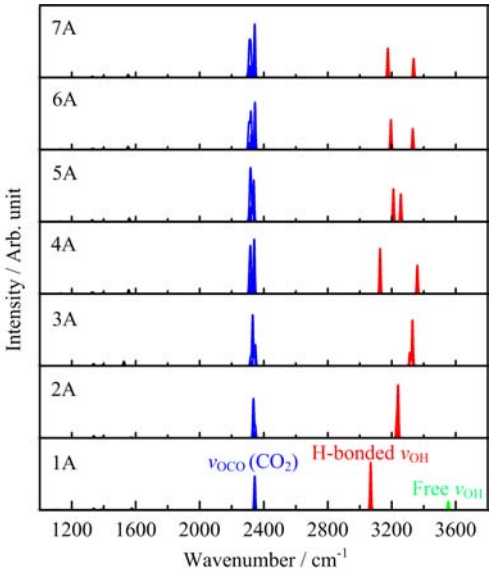

FIG. 9 Simulated IR spectra of the lowest-lying isomers of $H^+(CH_3OH)(CO_2)_n$ (n=1−7). Assignments of free O-H stretching, H-bonded O-H stretching, and O-C-O stretching for CO_2 unit are indicated in green, red, and blue, respectively.

IV. CONCLUSION

The effect of solvation on the conformation of protonated methanol, $H^+(CH_3OH)$, has been studied by adding one CO_2 molecule at a time. Quantum chemical calculations of the $[H^+(CH_3OH)(CO_2)_n]^+$ (n=1−7) clusters indicate that the first solvation shell of the OH groups is completed at n=3 or 4. Besides H-bond interaction, the $C_{CO_2}\cdots O_{CO_2}$ intermolecular interaction is also responsible for the stabilization of the larger clusters. The transfer of the proton from methanol onto CO_2 with the formation of the $OCOH^+$ moiety might be unfavorable in the early stage of solvation process. Simulated IR spectra reveal that vibrational frequencies of free O−H stretching, H-bonded O−H stretching, and O−C−O stretching of CO_2 unit afford the sensitive probe for exploring the solvation of protonated methanol by carbon dioxide. The combination of IRPD technique and theoretical modeling thus provides a vivid physical picture about how carbon dioxide solvates the protonated methanol.

V. ACKNOWLEDGMENTS

This work was supported by the National Natural Science Foundation of China (No.21273232 and No.21327901), the Key Research Program of the Chinese Academy of Science (No.KGZD-EW-T05). Ling Jiang acknowledges Hundred Talents Program of Chinese Academy of Sciences and Collaborative Innovation Center of Chemistry for Energy and Materials.

DOI:10.1063/1674-0068/28/cjcp1507146

[1] S. R. Gadre, S. D. Yeole, and N. Sahu, Chem. Rev. **114**, 12132 (2014).
[2] A. Fujii and K. Mizuse, Int. Rev. Phys. Chem. **32**, 266 (2013).
[3] S. Heinbuch, F. Dong, J. J. Rocca, and E. R. Bernstein, J. Chem. Phys. **125**, 154316 (2006).
[4] T. Habteyes, L. Velarde, and A. Sanov, J. Chem. Phys. **126**, 154301 (2007).
[5] N. Stafford, Nature **448**, 526 (2007).
[6] S. Balasubramanian, A. Kohlmeyer, and M. L. Klein, J. Chem. Phys. **131**, 144506 (2009).
[7] K. S. Thanthiriwatte, J. R. Duke, V. E. Jackson, A. R. Felmy, and D. A. Dixon, J. Phys. Chem. A **116**, 9718 (2012).
[8] K. H. Lemke and T. M. Seward, Chem. Phys. Lett. **573**, 19 (2013).
[9] Y. Danten, T. Tassaing, and M. Besnard, J. Phys. Chem. A **109**, 3250 (2005).
[10] A. Muraoka, Y. Inokuchi, N. Nishi, and T. Nagata, J. Chem. Phys. **122**, 094303 (2005).
[11] A. Muraoka, Y. Inokuchi, N. I. Hammer, J. W. Shin, M. A. Johnson, and T. Nagata, J. Phys. Chem. A **113**, 8942 (2009).
[12] Y. Inokuchi, Y. Kobayashi, A. Muraoka, T. Nagata, and T. Ebata, J. Chem. Phys. **130**, 154304 (2009).
[13] B. Bandyopadhyay, O. Kostko, Y. Fang, and M. Ahmed, J. Phys. Chem. A **119**, 4083 (2015).
[14] S. Kashtanov, A. Augustson, J. E. Rubensson, J. Nordgren, H. Agren, J. H. Guo, and Y. Luo, Phys. Rev. B **71**, 104205 (2005).
[15] K. R. Wilson, M. Cavalleri, B. S. Rude, R. D. Schaller, T. Catalano, A. Nilsson, R. J. Saykally, and L. G. M. Pettersson, J. Phys. Chem. B **109**, 10194 (2005).
[16] M. J. Frisch, G. W. Trucks, H. B. Schlegel, G. E. Scuseria, M. A. Robb, J. R. Cheeseman, G. Scalmani, V. Barone, B. Mennucci, G. A. Petersson, H. Nakatsuji, M. Caricato, X. Li, H. P. Hratchian, A. F. Izmaylov, J. Bloino, G. Zheng, J. L. Sonnenberg, M. Hada, M. Ehara, K. Toyota, R. Fukuda, J. Hasegawa, M. Ishida, T. Nakajima, Y. Honda, O. Kitao, H. Nakai, T. Vreven, J. A. Jr. Montgomery, J. E. Peralta, F. Ogliaro, M. J. Bearpark, J. Heyd, E. N. Brothers, K. N. Kudin, V. N. Staroverov, R. Kobayashi, J. Normand, K. Raghavachari, A. P. Rendell, J. C. Burant, S. S. Iyengar, J. Tomasi, M. Cossi, N. Rega, N. J. Millam, M. Klene, J. E. Knox, J. B. Cross, V. Bakken, C. Adamo, J. Jaramillo, R. Gomperts, R. E. Stratmann, O. Yazyev, A. J. Austin, R. Cammi, C. Pomelli, J. W. Ochterski, R. L. Martin, K. Morokuma, V. G. Zakrzewski, G. A. Voth, P. Salvador, J. J. Dannenberg, S. Dapprich, A. D. Daniels, O. Farkas, J. B. Foresman, J. V. Ortiz, J. Cioslowski, and D. J. Fox, *Gaussian 09, Rev A.02,*, Wallingford CT: Gaussian, Inc., (2009).
[17] M. Okumura, L. I. Yeh, and Y. T. Lee, J. Chem. Phys. **83**, 3705 (1985).
[18] E. J. Bieske and O. Dopfer, Chem. Rev. **100**, 3963 (2000).
[19] N. R. Walker, R. S. Walters, and M. A. Duncan, New J. Chem. **29**, 1495 (2005).
[20] T. R. Rizzo, J. A. Stearns, and O. V. Boyarkin, Int. Rev. Phys. Chem. **28**, 481 (2009).
[21] K. R. Asmis and D. M. Neumark, Acc. Chem. Res. **45**, 43 (2012).
[22] A. B. Wolk, C. M. Leavitt, E. Garand, and M. A. Johnson, Acc. Chem. Res. **47**, 202 (2014).
[23] G. E. Douberly, A. M. Ricks, B. W. Ticknor, and M. A. Duncan, J. Phys. Chem. A **112**, 950 (2008).
[24] L. Jiang, T. Wende, R. Bergmann, G. Meijer, and K. R. Asmis, J. Am. Chem. Soc. **132**, 7398 (2010).
[25] T. Wende, M. Wanko, L. Jiang, G. Meijer, K. R. Asmis, and A. Rubio, Angew. Chem. Int. Ed. **50**, 3807 (2011).

DOI:10.1063/1674-0068/28/cjcp1507146